ChemComm

COMMUNICATION

View Article Online
View Journal | View Issue

Cite this: *Chem. Commun.*, 2016, 52, 5558

Received 10th February 2016,
Accepted 22nd March 2016

DOI: 10.1039/c6cc01290f

www.rsc.org/chemcomm

Competing antiferromagnetic orders in the double perovskite Mn_2MnReO_6 (Mn_3ReO_6)†

A. M. Arévalo-López, F. Stegemann and J. P. Attfield*

The new double perovskite Mn_2MnReO_6 has been synthesised at high pressure. Mn^{2+} and Re^{6+} spins order antiferromagnetically through two successive transitions that are coupled by magnetoelastic effects, as order of the Mn spins at 109 K leads to lattice distortions that reduce frustration prompting Re order at 99 K.

Double perovskites $A_2BB'O_6$ with ordering of B/B′ transition metal cations on the ABO_3 perovskite-type lattice are an important group of oxide materials.[1] Some examples such as Sr_2FeMoO_6 and Sr_2FeReO_6 are ferrimagnetic, spin-polarised conductors with large low-field tunnelling magnetoresistances.[2] Many other double perovskites have antiferromagnetic ground states that may be frustrated due to the tetrahedral geometry of the B and B′ sublattices,[3,4] leading to a spin liquid ground state in Ba_2YMoO_6.[5]

The A^{2+} (= Ca, Sr, Ba, Pb) cations in double perovskites synthesised at ambient pressure are relatively large and non-magnetic. However, perovskites with only the smaller high spin Mn^{2+} ion at the A sites have recently been synthesised at high pressure and temperature conditions, introducing additional magnetic functionality. $MnVO_3$ perovskite is metallic due to itinerancy of the V^{4+} $3d^1$ states, as found in $CaVO_3$ and $SrVO_3$, but also has coexisting helimagnetic order of localised $S = 5/2$ Mn^{2+} spins.[6] The double perovskite Mn_2FeSbO_6 also has low temperature incommensurate antiferromagnetic Mn spin order.[7] Mn_2FeReO_6, also recently discovered through high pressure synthesis,[8,9] is particularly notable as it has a high Curie temperature (520 K), ferrimagnetic Fe^{3+}/Re^{5+} spin order, and negative tunnelling magnetoresistance like other A_2FeReO_6 double perovskites. The Mn^{2+} spins enhance the bulk magnetisation giving a record value for transition-metal double perovskites,[8] however, a further Mn magnetic ordering transition at 75 K frustrates and cants Fe^{3+} and Re^{5+} spins, resulting in a novel switch from negative to large positive magnetoresistances at low temperatures. Mn_2FeReO_6 was the first example of a double perovskite with magnetic transition metal ions at all of the cation sites. Here we have investigated whether Fe can be replaced by Mn and we report the synthesis and properties of a new double perovskite Mn_2MnReO_6 (Mn_3ReO_6) which shows successive antiferromagnetic ordering transitions for Re and Mn spins at 99 and 109 K respectively.

10–20 mg samples of Mn_2MnReO_6 were synthesised from a stoichiometric mixture of Mn_3O_4 and ReO_2 in a Pt capsule at 8 GPa and 1400 °C in a Walker-type multi-anvil press. The best polycrystalline product was highly phase pure with traces of MnO (<3 wt%) also observed. Small single crystals were separated from the walls of the capsule from one run and used for structure determination. Results are summarised in Table 1 and further details of the single crystal analysis and powder X-ray and neutron studies are in ESI.†

Mn_2MnReO_6 has a monoclinic double perovskite structure like those of A_2MnReO_6 (A = Ca and Sr) analogues.[10,11] A small antisite disorder (3.7%) for Mn/Re at B/B′ sites was observed in the single crystal, showing that the degree of cation ordering is very high. Bond valence sum (BVS) calculations in Table 1 show that the charge distribution is $Mn_2^{2+}Mn^{2+}Re^{6+}O_6$, in contrast to that of $Mn_2^{2+}Fe^{3+}Re^{5+}O_6$. The crystal structure is substantially distorted due to the small Mn^{2+} cations at the A sites. The ideal 12-coordination of the Mn_A site is split into four short (2.10–2.16 Å), four medium (2.61–2.79 Å) and four long (3.33–3.56 Å) Mn_A–O distances. The four short bonds create a distorted tetrahedral environment around Mn_A. The Mn_BO_6 and ReO_6 octahedra are also distorted, with ReO_6 showing a small tetragonal compression (two 1.88 and four 1.93–1.97 Å bonds) consistent with Jahn–Teller distortion from orbital order of the $5d^1$ Re^{6+} ions. Large tilts of the octahedra are observed, with Mn_B–O–Re angles of 135–140° deviating far from the ideal 180° value.

Magnetic susceptibility measurements in Fig. 1 show that Mn_2MnReO_6 is Curie–Weiss paramagnetic at high temperatures. A fit to the inverse susceptibility gives a Weiss temperature of $\theta = -147(1)$ K, showing that antiferromagnetic exchange

Centre for Science at Extreme Conditions (CSEC) and School of Chemistry, University of Edinburgh, Edinburgh EH9 3FD, UK. E-mail: j.p.attfield@ed.ac.uk

† Electronic supplementary information (ESI) available: Experimental details, plots and analysis of X-ray and neutron diffraction data. Open data for this article are at http://dx.doi.org/10.7488/ds/1359. See DOI: 10.1039/c6cc01290f

Table 1 X-ray single crystal refinement results (atomic coordinates, equivalent thermal B-factors, BVS's, and selected bond lengths) for Mn_2MnReO_6 at 120 K (space group $P2_1/n$; a = 5.2708(3) Å, b = 5.3869(4) Å, c = 7.7100(5) Å; β = 90.097(5)°)

	x	y	z	$B_{eq.}$ (Å^2)	BVS
Mn_A	0.5011(1)	0.9516(2)	0.2429(1)	0.68(2)	2.0
Mn_B[a]	1/2	1/2	0	0.29(1)	2.3
Re[a]	0	0	0	0.44(2)	5.9
O1	0.1212(5)	0.0707(7)	0.2366(3)	0.59(6)	2.0
O2	0.6906(5)	0.1725(5)	0.0577(3)	0.81(6)	2.1
O3	0.8462(5)	0.7020(5)	0.0713(3)	0.75(6)	2.0

Bond lengths (Å)

Mn_B–O1 (×2)	2.164(2)	Re–O1 (×2)	1.969(2)
Mn_B–O2 (×2)	2.078(2)	Re–O2 (×2)	1.930(2)
Mn_B–O3 (×2)	2.194(3)	Re–O3 (×2)	1.881(3)
Mn_A–O1	2.103(1)	Mn_A–O2	2.614(2)
Mn_A–O1	2.157(1)	Mn_A–O3	2.622(3)
Mn_A–O2	2.111(1)	Mn_A–O3	2.125(3)
Mn_A–O2	2.694(2)	Mn_A–O3	2.787(3)
Mn_A–O1	3.331(2)	Mn_A–O1	3.400(1)
Mn_A–O2	3.561(2)	Mn_A–O3	3.562(2)

Angles (°)

		Mn_B–O1–Re	137.7(2)
Mn_B–O2–Re	140.2(2)	Mn_B–O3–Re	135.2(1)

[a] Mn_B/Re antisite disorder = 3.7(4)%.

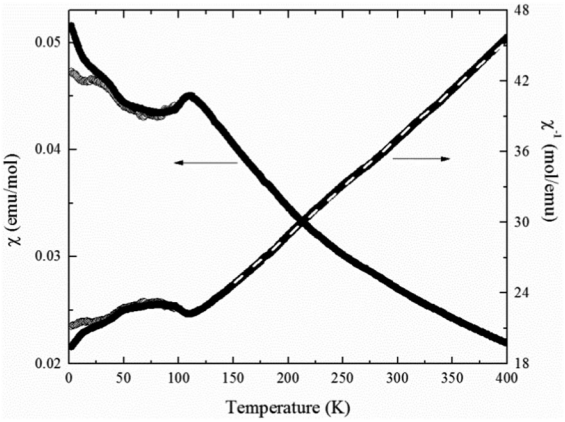

Fig. 1 Temperature evolution of the direct and inverse magnetic susceptibilities of Mn_2MnReO_6 under a 0.5 T field showing the 109 K spin ordering transition (open/filled points are ZFC/FC data). The Curie–Weiss fit to the inverse ZFC data is shown as a broken line.

interactions are dominant, and a paramagnetic moment of μ_{eff} = 4.9(1) μ_B per transition metal ion, close to the predicted spin-only value of 5.20 μ_B for $Mn_2^{2+}Mn^{2+}Re^{6+}O_6$. The susceptibility maximum at 109 K evidences an antiferromagnetic spin ordering, and a change of slope at 99 K is consistent with the second magnetic transition revealed by neutron diffraction below. Divergence of zero field cooled (ZFC) and field cooled (FC) susceptibilities below ~40 K may evidence a trace of the ferrimagnetic impurity Mn_3O_4, although this was not seen in the powder diffraction patterns. No magnetic or structural anomalies from Mn_2MnReO_6 are apparent in the neutron data near 40 K.

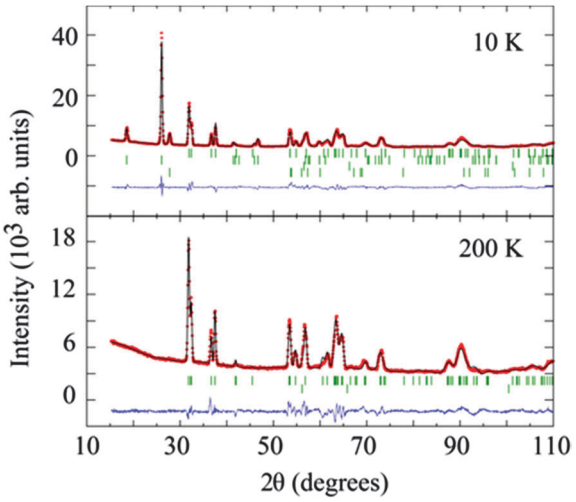

Fig. 2 Fits to powder neutron diffraction data for Mn_2MnReO_6 at 10 and 200 K. The nuclear structures of Mn_2MnReO_6 (upper reflection markers) and MnO (1 wt%; lower markers) are fitted to the 200 K data. Magnetic structures for both phases are additionally fitted to the 10 K pattern.

Four high pressure products were combined to give a ~70 mg sample of Mn_2MnReO_6 for neutron powder diffraction to investigate the low temperature properties further. Fig. 2 displays the profiles at 10 and 200 K. Rietveld refinements showed that the monoclinic $P2_1/n$ structure is retained down to the lowest measured temperature of 10 K. A greater degree (12%) of Mn_B/Re antisite disorder was observed than in the single crystal, this probably reflects slight compositional variations between the combined polycrystalline samples.

The onset of antiferromagnetic order in Mn_2MnReO_6 is marked by the appearance of several magnetic diffraction peaks below 109 K. However, the temperature variation of the magnetic intensities (see inset to Fig. 3) shows that a further spin transition occurs at 99 K. All of the Mn_2MnReO_6 magnetic peaks are indexed

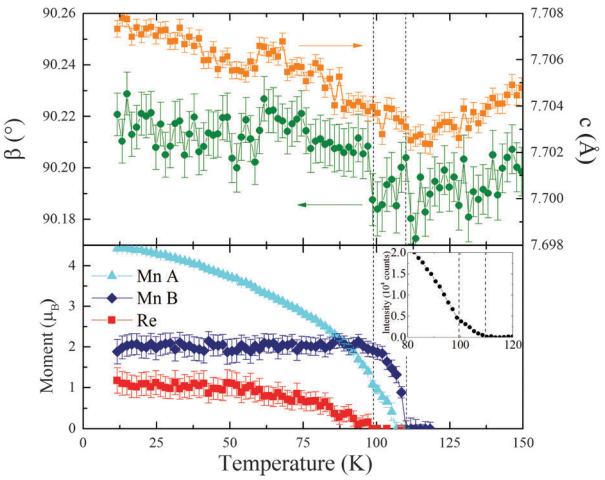

Fig. 3 Temperature evolution of the unit cell parameters c and β (upper panel) and magnetic moments (lower panel) for Mn_2MnReO_6, showing the T_{Re} = 99 and T_{Mn} = 109 K spin transitions. The inset shows the variation of the (1/2 1/2 1) magnetic peak intensity around the transitions.

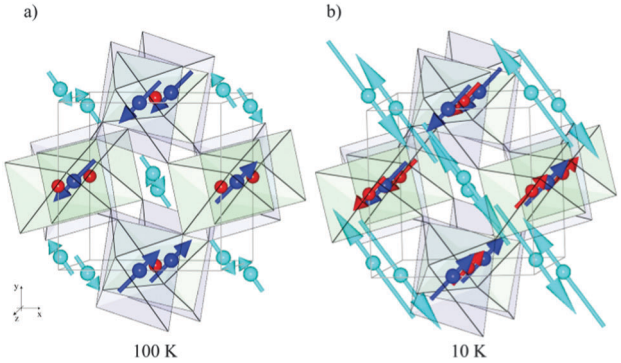

Fig. 4 (a) Crystal and magnetic structures of Mn_2MnReO_6 shown for the nuclear $P2_1/n$ cell at (a) 100 K with order of only Mn_A and Mn_B moments, and (b) 10 K showing order of all spins. $Mn_A/Mn_B/Re$ are cyan/blue/red spheres.

by the $\boldsymbol{k}$ = (1/2 1/2 0) propagation vector. Analysis of the 10 K magnetic neutron data reveals that all of the moments lie in the *ab*-plane (details are in ESI†). The Mn_A, Mn_B and Re spins form three independent antiferromagnetic sublattices. Initial refinements showed that Mn_A and Mn_B spins are approximately perpendicular, and best fits were obtained when they were constrained to be parallel to [110] and [1$\bar{1}$0] directions respectively. Re moments are small and were constrained to be collinear with Mn_B spins; other directions did not improve the fit. The thermal evolution of the refined model shows that the Mn_A and Mn_B spins order at the upper transition at T_{Mn} = 109 K, whereas Re moments order separately at T_{Re} = 99 K. Thermal variations of the ordered moments and lattice strains are shown in Fig. 3, and magnetic structures in the two regimes are in Fig. 4.

The (upper) magnetic ordering temperature of 109 K for Mn_2MnReO_6 is comparable to those of 110 and 120 K for Ca_2MnReO_6 and Sr_2MnReO_6.[10] However the latter materials are both ferrimagnets, with simultaneous $\boldsymbol{k}$ = (0 0 0) order of Mn and Re spins observed in a neutron diffraction study of Sr_2MnReO_6.[11] Hence the $\boldsymbol{k}$ = (1/2 1/2 0) antiferromagnetism of Mn_2MnReO_6 with separate ordering transitions for the two transition metal B-site sublattices, which is very unusual in double perovskites, shows that interactions of B-site spins with Mn_A moments are significant and suppress the Re spin order. Antiferromagnetic order within B/B′ tetrahedral networks is frustrated in double perovskites, but Mn_2MnReO_6 also has frustrated interactions between A and B/B′ cations, as each Mn_A spin has 2 up and 2 down spins from the surrounding Mn_B and Re spin tetrahedra, and each B/B′-site spin has 4 up and 4 down Mn_A spins as neighbours. This results in perpendicular alignment of A and B/B′ spins to maximise antisymmetric Dzyaloshinskii–Moriya interactions. The relative strengths of the competing antiferromagnetic orders are revealed by the moment variations in Fig. 3. Below T_{Mn} = 109 K the ordered Mn_B moment rises rapidly up to 1.9 μ_B at 99 K whereas Mn_A increases more slowly to 1.1 μ_B, showing that dominant Mn_B order partially frustrates Mn_A spins and fully frustrates Re order. However, below T_{NA} = 99 K further Mn_B order is frustrated as the moment saturates at 2.0 μ_B while less-frustrated Mn_A and Re spins rise to saturated moments of 4.5 and 1.0 μ_B, close to ideal values of 5 and 1 μ_B respectively.

Although the magnetic structure of Mn_2MnReO_6 appears frustrated as discussed above, this is not reflected by the ratio $-\theta/T_{NB}$ = 1.3 which is close to unity. This demonstrates that monoclinic lattice distortion relieves much of the frustration by breaking the degeneracy of Mn_B–O–Re superexchange interactions. Further evidence comes from observed anomalies in lattice parameters at the two transitions as shown in Fig. 3 and ESI.† The change in thermal expansion of *c* from positive to negative on cooling through T_{Mn} increases the monoclinic distortion as $a, b < c/\sqrt{2}$. This reduces frustration further and so is the likely factor that drives the long range order of Re spins at 99 K. The proximity of the two antiferromagnetic transitions thus arises from magnetoelastic effects. Re spin order further changes the magnetoelastic coupling as evidenced by the anomaly in β at T_{Re}.

In conclusion, Mn_2MnReO_6 is the first example of a $A_2BB'O_6$ double perovskite with antiferromagnetically ordered transition metal spins at all cation sites. Frustration between the three antiferromagnetic sublattices results in perpendicular orientations of the A and B/B′ spins and long range magnetic ordering through two successive antiferromagnetic transitions. These show an unusual coupling through magnetoelastic effects, as order of the Mn spins at T_{Mn} = 109 K leads to lattice distortions that reduce frustration leading to Re spin order at T_{Re} = 99 K. Around 650 $A_2BB'O_6$ double perovskite oxides are previously reported[1] but Mn_2FeReO_6 and Mn_2MnReO_6 are the only two with magnetic transition metal ions at all sites, and both have novel magnetic properties due to the presence of A-site Mn^{2+}, so it is likely that many more interesting 'all transition metal' double perovskites will be accessible through high pressure synthesis.

We thank EPSRC, STFC and the Royal Society for support and provision of ILL beamtime, and Dr C. Ritter for assistance with data collection.

Notes and references

1 S. Vasala and M. Karppinen, *Prog. Solid State Chem.*, 2014, **43**, 1.
2 D. Serrate, J. M. De. Teresa and M. R. Ibarra, *J. Phys.: Condens. Matter*, 2007, **19**, 023201.
3 J.-W. G. Bos and J. P. Attfield, *Phys. Rev. B: Condens. Matter Mater. Phys.*, 2004, **70**, 174434.
4 C. M. Thompson, C. A. Marjerrison, A. Z. Sharma, C. R. Wiebe, D. D. Maharaj, G. Sala, R. Flacau, A. M. Hallas, Y. Cai, B. D. Gaulin, G. M. Luke and J. E. Greedan, *Phys. Rev. B: Condens. Matter Mater. Phys.*, 2016, **93**, 014431.
5 J. P. Carlo, J. P. Clancy, T. Aharen, Z. Yamani, J. P. C. Ruff, G. J. Van Gastel, G. E. Granoth, J. E. Greedan, H. A. Dabkowska and B. D. Gaulin, *Phys. Rev. B: Condens. Matter Mater. Phys.*, 2011, **84**, 100404.
6 M. Markkula, A. M. Arévalo-López, A. Kusmartseva, J. A. Rodgers, C. Ritter, H. Wu and J. P. Attfield, *Phys. Rev. B: Condens. Matter Mater. Phys.*, 2011, **84**, 094450.
7 A. J. Dos Santos-García, C. Ritter, E. Solana-Madruga and R. Sáez-Puche, *J. Phys.: Condens. Matter*, 2013, **25**, 206004.
8 A. M. Arevalo-Lopez, G. M. McNally and J. P. Attfield, *Angew. Chem., Int. Ed.*, 2015, **54**, 12074.
9 M.-R. Li, M. Retuerto, Z. Deng, P. W. Stephens, M. Croft, Q. Huang, H. Wu, X. Deng, G. Kotliar, J. Sanchez-Benitez, J. Hadermann, D. Walker and M. Greenblatt, *Angew. Chem., Int. Ed.*, 2015, **54**, 12069.
10 H. Kato, T. Okuda, Y. Okimoto, Y. Tomioka, K. Oikawa, T. Kamiyama and Y. Tokura, *Phys. Rev. B: Condens. Matter Mater. Phys.*, 2004, **69**, 184412.
11 G. Popov, V. Lobanov, E. V. Tsiper, M. Greenblatt, E. N. Caspi, A. Borissov, V. Kiryukhin and J. W. Lynn, *J. Phys.: Condens. Matter*, 2004, **16**, 135.